Green Chemistry

Accepted Manuscript

ROYAL SOCIETY OF CHEMISTRY

www.rsc.org/greenchem

Table of contents entry

Engineering the filamentous, N_2-fixing cyanobacteria as a cellular factory to produce and secret a cyclic hydrocarbon fuel using atmospheric gases (CO_2, N_2), water, and sunlight.

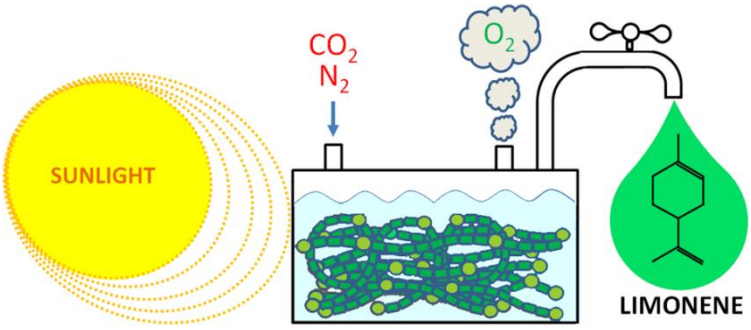

CYANOFACTORY FOR BIOFUELS

Engineering Cyanobacteria for Production of a Cyclic Hydrocarbon from CO_2 and H_2O

Charles Halfmann[a], Liping Gu[a], and Ruanbao Zhou[a*]

Received (in XXX, XXX) Xth XXXXXXXXX 20XX, Accepted Xth XXXXXXXXX 20XX

DOI: 10.1039/b000000x

Abstract

Cyclic hydrocarbons are a critical component of petroleum fuels. However, biofuels produced by current biochemical and thermochemical processes contain little cyclic hydrocarbons, which can only provide the requisite performance characteristics with the addition of petroleum fuels. Limonene ($C_{10}H_{16}$) is a cyclic monoterpene that possesses attractive characteristics as a biodiesel and jet fuel. Current strategies for harvesting limonene from plant biomass require arable land, high energy inputs, inefficient multiple-step processes, and the release CO_2 as a greenhouse gas. This research focuses on a direct photons-to-product approach in biofuel production by metabolically engineering a cyanobacterium as cellular machinery to over-produce and secrete valuable compounds using CO_2, mineralized H_2O, and light. As a proof of concept, we have engineered the filamentous, nitrogen-fixing cyanobacterium *Anabaena* sp. PCC 7120 to synthesize and secrete limonene by transferring in a plant limonene synthase gene (*lims*) from Sitka spruce. Our data revealed that limonene produced by the engineered cyanobacterium was secreted across the cell membrane and volatilized into the headspace, allowing for easy separation of the target compound from the culture biomass. Furthermore, a synthetic DXP operon (*dxs-ipphp-gpps)* encoding three rate-limiting enzymes from the MEP pathway was co-

expressed with *lims* to re-route carbon flux from the Calvin cycle into limonene synthesis. Under higher light (150 $\mu E \cdot m^{-2} \cdot s^{-1}$), we observed a 6.8-fold increase in limonene yield and an 8.8-fold increase in the maximum limonene production rate when expressing the DXP operon in conjunction with *lims*, compared to *lims* alone; and achieved a maximum production rate of 3.6±0.5 μg limonene$\cdot L^{-1} \cdot O.D.^{-1} \cdot hr^{-1}$. This limonene-producing *Anabaena* has about three times higher photosystem II activity than its wild-type. These results demonstrated that increasing light intensity and metabolic flux improves limonene productivity in the engineered cyanobacteria. We envision that the platform of using N_2-fixing cyanobacteria as a cellular factory, and CO_2 and N_2 as sustainable feedstocks can be applicable for the production of a wide range of commodity chemicals and drop-in-fuels.

Broader Context

The world is currently facing two pressing problems: fossil fuel depletion and global climate change due to elevated CO_2 emissions. To solve these two critical problems, biofuel production from corn and sugarcane has given hope in mitigating the human carbon footprint, while decreasing our consumption of fossil fuels. Photosynthetic organisms including plants, algae, and cyanobacteria utilize light energy to convert CO_2 into fixed carbon, which is stored as chemical energy in their biomass. To unlock the energy from plant biomass requires long growing seasons, harvesting, industrial processing, and competition with food crops for land use. Photosynthetic microorganisms hold a distinct advantage in biofuel production over plants, given their faster growth rates, higher photosynthetic efficiencies, and simpler nutrient requirements. Engineered cyanobacteria with re-wired metabolic pathways have recently been designed through genetic engineering, and they possess the unique ability to synthesize new chemicals and biofuels, which are secreted from their cells. In this paper, we report the results of using a bench-scale "cyanofactory" for the production of cyclic hydrocarbon limonene from atmospheric gases, mineralized water, and light.

Introduction

Terpenes are a large and diverse class of long-chained alkenes that are naturally synthesized in animals, plants, and bacteria.[1, 2] They play important roles in hormone and pigment biosynthesis, cell membrane maintenance, and are the main constituents of many essential oils and volatiles in plants.[3-6] Limonene is a naturally occurring cyclic monoterpene found mainly in the rinds of citrus fruits, and has important applications in jet fuels[7], flavoring, and pharmaceuticals.[8] Its immiscibility in water and low freezing point makes it an ideal candidate as a 3rd generation jet-fuel and biodiesel.[9] Due to its cyclic structure, this compound has the potential to be further functionalized through cyclopropanation, to increase its energetic content and enhance its value as a fuel.[10] Limonene has also been extensively researched as a possible therapeutic agent, due to its anti-inflammatory and anti-carcinogenic properties.[11-13] Global limonene production is far behind the arising demands for biofuels. Approximately 50,000 metric tons of limonene are extracted per year, primarily from the residue of harvested citrus fruits.[8] However, limonene extraction from citrus rinds involves mechanical pressurizing and distillation, making production of this compound an energy intensive and costly process.

In the last decade, advancements in systems biology have increased our understanding of the complex cellular systems that generate biofuels from carbon-based feedstocks, and have opened the door to possibilities of using "cellular factories" for large-scale biofuel production. Most microbes already possess the biochemical pathways needed to produce biofuels and commodity chemicals or their precursors, but there are certain crucial components which restrict the organism to synthesize them efficiently, such as low expressions and/or low activities of the rate-limiting enzymes within the pathways. To overcome these bottlenecks, endogenous anabolic pathways have been synthetically re-wired for chemical production using genetic engineering.[14, 15] Microbial terpene synthesis has already been reported from genetically modified strains of *Escherichia coli*, which synthesize terpenes from

reduced carbon sources, such as glucose.[16-20] However, using reduced carbon feedstocks from harvested plant material for microbial biofuel production is an added cost factor that puts these approaches at an economic disadvantage compared to photosynthetic systems that utilize CO_2 directly. Here, we focus on the photosynthetic production of limonene from a cyanobacterium using CO_2, H_2O, and light. Cyanobacteria are ideal hosts for producing high value chemicals, due to their fast growth rates, ease of genetic manipulation, minimal growth requirements, and their ability to synthesize compounds using CO_2, a greenhouse gas already abundant in the atmosphere. Unicellular species of cyanobacteria, such as *Synechocystis* sp. PCC 6803 and *Synechococcus* sp. PCC 7942, have been genetically engineered to produce a wide range of compounds, including isoprene,[21] ethylene,[22, 23] 2,3-butanediol,[24] isobutyraldehyde,[25] and sucrose.[26] *Anabaena* sp. PCC 7120 (hereinafter referred to as *Anabaena*) is a filamentous, nitrogen-fixing cyanobacterium which has previously been engineered for hydrogen production.[27] Unlike the two unicellular cyanobacteria above, *Anabaena* possesses the ability to assimilate dinitrogen gas (N_2) into organic nitrogen in compartmentalized cells called heterocysts, which are located along the filament. This gives *Anabaena* a special advantage in biofuel production, since supplied nitrogen currently imposes a predominant cost factor in large scale biofuel strategies.[28, 29]

In cyanobacteria, the main biosynthetic pathway for terpene synthesis is the 2-*C*-methyl-D-erythritol 4-phosphate/1-deoxy-D-xylulose 5-phosphate pathway, or MEP/DXP pathway (Fig. 1). Cyanobacteria possess an endogenous MEP pathway for the synthesis of photosynthetic pigments, as well as plastoquinones involved in electron transport.[30] In the MEP pathway, pyruvate and glyceraldehyde-3-phosphate (GAP) are condensed and brought through a series of enzymatic reactions, eventually leading to the synthesis of isopentenyl diphosphate (IPP) and dimethylallyl diphosphate (DMAPP). Then, IPP and DMAPP further condense to create geranyl pyrophosphate (GPP), the direct precursor of all monoterpenes, including limonene. Although cyanobacteria possess an endogenous MEP pathway, they are missing limonene synthase (LimS), the enzyme that catalyzes the final reaction of

GPP to limonene. Here we seek to add to the cyanobacteria's genetic repertoire by heterologously expressing a plant LimS in *Anabaena* to enable the photosynthetic production of limonene. We further increased limonene production nearly seven fold by over-expressing three rate-limiting enzymes in the MEP pathway to pull more carbon flux towards limonene synthesis. Using these strategies, we successfully built a "cyanofactory" capable of producing and secreting limonene using atmospheric gases (CO_2 and N_2), light, and mineralized water. We envision this platform of using CO_2 and N_2 as a sustainable feedstock to be applicable for the production of a wide range of commodity chemicals and drop-in-fuels.

Results and Discussion

Expression of limonene synthase in *Anabaena*

We first sought to utilize the endogenous MEP pathway in *Anabaena* for the production of limonene using atmospheric CO_2 as a carbon feedstock. Although *Anabaena* possesses an endogenous MEP pathway to produce GPP, the precursor for limonene, it is missing limonene synthase (LimS), the enzyme that catalyzes the conversion from GPP to limonene. Thus, we introduced a limonene synthase gene (*lims*; Genbank accession no. DQ195275) from Sitka spruce (*Picea sitchensis*) to the cyanobacterium by cloning the ORF lacking the N-terminal plastid transit sequence into the replicating shuttle vector pZR1188 to create pLimS (Fig. 2A and Table 1). This truncated LimS was previously characterized as a limonene synthase through an *in vitro* enzymatic activity assay.[31] As illustrated in Fig. 2A, a $FLAG_2$ epitope tag was fused to the C-terminus of LimS for monitoring LimS-$FLAG_2$ protein expression in *Anabaena*. The LimS-$FLAG_2$ expression was driven by a dual *Anabaena* P_{nir}-P_{psbA1} promoter to maintain maximal protein expression constitutively in the cells. The construct pLimS was introduced into *Anabaena* through conjugation, and colonies that conferred resistance to neomycin were selected for testing LimS-$FLAG_2$ expression by Western blotting. As seen in Fig. 2B,

an expected 69 kDa protein was detected from immunoblotting with anti-FLAG antibodies in LimS (lane 2), but not in WT *Anabaena* (lane 1), suggesting that LimS-$FLAG_2$ was expressed in *Anabaena*.

Identification of limonene emitted from LimS *Anabaena* grown under CO_2 and light

Due to its hydrophobicity and volatility, limonene readily phase-separates from aqueous solutions and volatilizes, making its collection and identification from cyanobacteria cultures problematic. Bentley et al.[32,33] worked around this problem by sealing the bioreactor headspace of a growing culture with pure CO_2, which trapped volatilized compounds for analysis. Another method is adding a liquid solvent layer to the growth media, which rests on top of the culture surface and "milks" hydrophobic compounds excreted from the cells.[9,20] We developed an alternative method to identify and accurately quantify limonene being produced from the cells using an aerating system that allows for continuous limonene collection without inhibiting gas exchange between the culture fluid and the atmosphere. In our approach, a resin column is attached to the gas outflow of a culture flask that is bubbled with a steady stream of filtered air. As hydrophobic compounds are volatilized from the culture and pushed through the outflow, they are captured by the resin, which is then eluted with pentane and analyzed through GC-MS. Absorption tests of the commercial resin Supelpak 2SV (2SV) showed nearly a 100% recovery of 100 µg limonene by 100 mg resin from limonene-spiked *Anabaena* wild-type cultures (data not shown).

To determine whether the expressed LimS-$FLAG_2$ was functionally active in *Anabaena*, we cultivated the *Anabaena* bearing pLimS (LimS *Anabaena*), collected the volatile compounds emitted from the culture fluid through the 2SV column, and then analyzed them by GC-MS. Fig. 3 shows GC-MS chromatographs of WT *Anabaena*, LimS *Anabaena*, and a 5 ppm limonene standard. A prominent peak appears at 9.47 minutes in the LimS *Anabaena* chromatograph (Fig. 3B) but not in WT *Anabaena* (Fig. 3A). This peak was identified as limonene by comparing it to the MS spectra and retention time

of a limonene standard (Fig. 3C). No limonene was detected in the culture medium or homogenized cell extracts (data not shown), suggesting an efficient transfer of limonene from the growing culture to the headspace.

We employed a continuous growth and limonene recovery system to analyze the amounts of limonene produced from LimS *Anabaena* over a 14 day growth period. LimS *Anabaena* was grown under experimental growth conditions, with an initial culture set at 0.5 optical density at 700 nm ($O.D._{700\ nm}$) and fresh BG11 medium replaced on day 8 to ensure adequate nutrient conditions during the limonene production trial. To measure limonene production, the 2SV column fitted to each culture flask was replaced every two days, and volatiles from the resin samples were eluted with pentane and quantified by GC-MS. Our results showed that LimS *Anabaena* produced 12.7±0.4 µg limonene·L^{-1}·48 hr^{-1}, and these amounts increased over the duration of the growth period (Fig. 4B). Total limonene accumulation was measured at 114.3±3.9 µg·L^{-1} during 14 days of growth. Taken together, our GC-MS data indicated that the LimS expressed in *Anabaena* was functionally active and the engineered *Anabaena* strain was capable of producing and emitting limonene.

Creation of a synthetic operon to increase MEP pathway flux

Our GC-MS data proved that the expression of an exogenous plant LimS in *Anabaena* enables the cyanobacterium to consecutively synthesize and emit limonene via photosynthesis. We then developed a strategy to increase limonene production through further metabolic engineering of the cyanobacterium. To accomplish this, we first looked at the MEP pathway as a potential target for metabolic enhancement. In order to increase levels of reaction intermediates and ultimately boost carbon input towards limonene production, three key enzymes that represented "bottleneck" points in the synthesis of target intermediates in the pathway were over-expressed. As illustrated in Figure 1, 1-deoxy-D-xylulose 5-phosphate synthase (DXS) catalyzes the first step in terpene synthesis by

condensing pyruvate and GAP to create 1-deoxy-D-xylulose 5-phosphate (DXP). IPP:DMAPP isomerase (IDI) converts the reversible reaction of IPP to DMAPP by changing the location of a double bond on the IPP molecule. DMAPP and IPP are then condensed by GPP synthase (GPPS) to create GPP, a direct precursor used to produce limonene catalyzed by LimS. Previously, the over-expression of DXS and IPPHP (an IDI from *Haematococcus pluvialis*), along with a farnesyl pyrophosphate synthase (IspA from *E. coli*) resulted in a 3.6-fold increase in amorphadiene produced from an engineered strain of *E. coli*.[34] We followed this approach to specifically target these crucial reactions in limonene synthesis, and acquired a DXS (encoded by the gene *dxs* from *E. coli*; Genebank accession no. AF035440.1), IPPHP (encoded by the gene *ipphp1* from *Haematococcus pluvialis*; Genebank accession no. AF082325.1) and GPPS (encoded by the gene *Rv0989c* from *Mycoplasma tuberculosis*; Genbank access no. AFN48878.1) for co-expression with LimS in *Anabaena* for increased limonene production. These three genes were cloned downstream of LimS in pLimS to create a new construct, named pLimS-DXP (Fig. 2A). LimS-DXP *Anabaena* bearing pLimS-DXP plasmid was subjected to analyze differences in limonene productivity compared with LimS *Anabaena*.

Expression of a *dxs-ipphp-gpps* operon increases limonene yield in *Anabaena*

To test whether limonene influences *Anabaena* growth, 100 mL cultures of LimS, LimS-DXP, and WT *Anabaena* cells were set to an $O.D._{700\ nm}$ of 0.1 and grown in continuous air bubbling conditions, with fresh resin columns and BG11 medium refreshed every 5 days for a 15 day growth period. As shown in Fig. 4A, cell growth kinetics of LimS and LimS-DXP *Anabaena* were similar to the WT, suggesting little to no cell toxicity from limonene excreted across the cell membrane. A similar pattern was observed for chlorophyll content among the WT, LimS, and LimS-DXP *Anabaena* strains (data not shown). Under 50 $\mu E \cdot m^{-2} \cdot s^{-1}$ light conditions, the addition of the DXP operon with LimS

resulted in an approximate 2.3-fold increase in total limonene yield (Fig. 4B), with 31.2±0.9 µg limonene·L^{-1}produced during the first two days and reaching the highest yield during the last two days of the experiment (46.5±0.8 µg limonene·L^{-1}·48 hr^{-1}). Total limonene accumulation was 268.2±11.2 µg·L^{-1} for LimS-DXP *Anabaena* during the 14 day growth trial. This increase in yield and productivity was similar to that reported previously in engineered *E. coli*.[34] The results indicate that the expression of DXS, IPPHP, and GPPS diverts additional carbon into the MEP pathway for limonene synthesis, and ultimately improves final product yield.

To determine the production rate of limonene from each of the transgenic strains, aliquots of 500 µL cultures from the above experiment were collected at two-day intervals to assess chlorophyll concentration. Both LimS and LimS-DXP *Anabaena* displayed similar patterns for chlorophyll content (Fig. 4C) and culture density (data not shown) during 14 days of growth. Initial limonene production rates were measured to be 770.0±31.6 and 1853.1±67.1 ng limonene·d^{-1}·mg chl^{-1} for LimS and LimS-DXP *Anabaena*, respectively, but slowly decreased throughout the production trial (Fig. 4D), until it levelled out from days 3-14 for LimS and LimS-DXP *Anabaena*. We interpret this decrease in production rate to a reduction in the number of photons harvested by the cells, due to poor light penetration from an increased cell density in the culture flasks. This decrease in limonene production per mg of chlorophyll suggests that light energy plays an important role in maximizing biofuel synthesis in the engineered cyanobacterium.

Enhancement of photosystem II (PSII) activity by a new carbon sink

We hypothesized that forcing *Anabaena* to allocate more fixed carbon into the MEP pathway for limonene production would result in a positive feedback in the light reactions (PSI, PSII) for photochemical energy production. Since limonene establishes a new carbon channel in cyanobacterial anabolism, more ATP and NADPH would need to be created to drive the continuous synthesis of fixed

carbon in the Calvin cycle, in order to maintain normal cell growth and metabolism. This was tested by measuring photosynthetic oxygen evolution of WT, LimS, and LimS-DXP *Anabaena* in increasing light intensities. Previous experiments showed that oxygen production rates of WT, LimS, and LimS-DXP *Anabaena* were similar within the first 3 minutes of analysis (data not shown). However, we found that each strain differed in its overall O_2 production amount after 10-15 minutes, with LimS and LimS-DXP *Anabaena* exhibiting higher O2 saturation levels than WT *Anabaena* in the 250-1000 $\mu E \cdot m^{-2} \cdot s^{-1}$ light range (Fig. 5A). LimS-DXP *Anabaena* produced the most (over 20 nmol O_2 $mL^{-1} \cdot \mu g$ $chlorophyll^{-1}$), about three times higher than in the WT (Fig. 5A). These higher light ranges were well over the intensity used for our low light limonene production trials (50 $\mu E \cdot m^{-2} \cdot s^{-1}$, Fig. 4B), indicating that these engineered *Anabaena* strains had a possible higher capacity for limonene production under stronger light intensities. Previously, it was reported that increasing the light intensity from 50 to 600 $\mu E \cdot m^{-2} \cdot s^{-1}$ resulted in a 2-fold increase in ethylene production in an engineered *Synechocystis* 6803.[23] Indeed, reduction of self-shading by optimizing light conditions will be a critical step towards large-scale biofuel platforms using photosynthetic microorganisms.

Increasing light intensity improves limonene production in *Anabaena*

Previously, we found that the addition of the DXP operon with LimS resulted in an approximate 2.3-fold increase in total limonene yield (Fig. 4B) under low light (50 $\mu E \cdot m^{-2} \cdot s^{-1}$). To test the effects of increased light intensity on limonene production, LimS and LimS-DXP *Anabaena* were grown in high light (150 $uE \cdot m^{-2} \cdot s^{-1}$) from an initial $O.D._{700nm}$ of 0.05, and emitted limonene was measured after 4 days of growth, followed by measurements every two days for 12 days total (Fig. 5BCD). Increasing the light intensity 3-fold (from 50 $\mu E \cdot m^{-2} \cdot s^{-1}$ to 150 $\mu E \cdot m^{-2} \cdot s^{-1}$) resulted in an overall 2.6-fold increase in limonene yield for LimS-DXP *Anabaena* during the 12 day trial (Fig. 5B). Furthermore, the maximum limonene accumulation yield (173μg) during days 7-8 was 5-fold higher than that (35μg) in

low light intensity. At higher light, total limonene accumulation production (521μg) from LimS-DXP *Anabaena* was 6.8-fold higher than that (76μg) from LimS *Anabaena* during the 12 day trial. Additionally, the maximum limonene accumulation (173μg) from LimS-DXP *Anabaena* was 8.8-fold higher than that (19.6μg) from LimS *Anabaena* from days 7-8 (Fig. 5B, day 7-8). However, it was only 1.7-fold higher during the same time period in low light (data not shown). These results strongly support that stronger light intensity improves limonene productivity and the potential of LimS-DXP vs. LimS *Anabaena*. We achieved a maximum yield of 172.7±16.9 μg limonene·L^{-1}·48 hr^{-1} (Fig. 5B) and a maximum production rate of 3.6±0.5 μg limonene·L^{-1}·O.D.·hr^{-1} in LimS-DXP *Anabaena* (Fig. 5D). However, limonene production rate declined after 8 days (Fig. 5D), corresponding with an $O.D._{700nm}$ surpassing 1.0 in high light conditions (Fig. 5C). The observed increase in limonene productivity during high light conditions and the correlation between limonene production and optical density (cell density) emphasizes the importance of maintaining optimal light penetration into cultures throughout biofuel production periods. We would expect outdoor cultivars to exhibit even higher production rates and yield, where outdoor light intensity can reach 2000 μE·m^{-2}·s^{-1} at midday in summer, which is more than 13 times higher than the light intensity used in this limonene production trial.

Calculating limonene productivity in large-scale applications

We applied parameters from algae biomass production models[35,36] to calculated limonene productivity of LimS-DXP *Anabaena* in a large-scale application. Ideally, a limonene production facility in the Midwest would be located next to a 380 million liter·yr^{-1} ethanol plant, which would generate 275,000 metric tons of CO_2·yr^{-1} and provide enough low-grade heat to operate a 10 hectare greenhouse. Assuming a total enclosed photobioreactor (PBR) volume of 6.4 million L, 8 hours of sunlight·day^{-1}, and a growing season of 300 days, we calculated a productivity of 55.3 kg limonene annually from this system, given the current production rate of 3.6 μg limonene·L^{-1}·$O.D.^{-1}$·hr^{-1}, making large-scale

limonene production from cyanobacteria unrealistic at this stage in the engineering.

The cycling of CO_2 from a processing facility into an industrial PBR is one scenario to make large-scale limonene production from cyanobacteria an attractive option. If a ten-hectare facility could convert 1 % of the annual CO_2 emissions from one ethanol plant into limonene, it would theoretically produce 852.5 metric tons of limonene·yr^{-1} (1013674 L·yr^{-1} or about 2% of the global market), and require a production rate 55.5 mg limonene·L^{-1}·hr^{-1}. This productivity would be 5-fold higher than the reported ethanol productivities from Joule Unlimited,[37] but only about 1.5-fold higher than the reported sucrose productivity by engineered cyanobacteria.[26] This production rate (55.5 mg limonene·L^{-1}·hr^{-1}) would also require the cyanobacteria to commit roughly 5-15 % of its daily fixed carbon to limonene, given previous studies on cyanobacteria carbon fixation rates (375-1230 mg dry weight ·L^{-1}·hr^{-1}).[38,39] The assumed daily requirement of 5-15% fixed carbon to limonene is lower than the harvest index (0.17-0.62) of several crops.[40] Factoring in rough cost estimates for capital, labor, and operation, a total production cost of \$1.30-1.50·L^{-1} limonene is possible (see cost calculations in Materials & Methods), compared to the current market price of \$4-5·L^{-1}.

Future challenges in cyanobacterial biofuel production

Our findings unveil a proof-of concept in using cyanobacteria for synthesizing and secreting limonene using CO_2, H_2O, and light. However, this and similar systems that utilize photosynthetic microorganisms to synthesize biofuels need further optimization to be competitive with petroleum and biofuel alternatives. Low productivities, inefficient product separation processes, and high capital costs are the key areas that are holding back large-scale production from commercialization. There is also the potential of cell toxicity from higher biofuel titers in future engineered strains, which would ultimately reduce biofuel yield. Resources such as natural sunlight, flue gas, and wastewater will likely need to be utilized for industrial facilities to become economically sustainable. Photobioreactors

designed to optimize CO_2, temperature, nutrients, and light will also need to be used to keep biofuel production at optimal rates. Furthermore, biomass-biofuel separation techniques must be engineered to collect the biofuel efficiently and alleviate cell toxicity.

One of the metabolic engineering challenges of microbial biofuel production is overcoming the cells innate regulation of its natural biosynthetic pathways, and forcing energy into creating an unnatural product. Cyanobacteria exhibit a myriad of sophisticated control systems that govern energy and carbon partitioning in many biosynthetic networks, including the MEP pathway. One approach to bypass these control systems is by introducing an alternate but functional biofuel synthesis pathway, which would attenuate host control and allow for increased production. This has already been demonstrated by introducing the alternative mevalonate pathway (MVA) from *Saccharomyces cerevisiae* into an engineered *E. coli,* which resulted in limonene titers of up to 435 mg limonene·L^{-1} culture.[20]

Several species of cyanobacteria, including *Anabaena* 7120, store significant amounts of energy-rich glycogen in granule compartments in the cytoplasm. One tactic to unlock this stored carbon for biofuel production involves the inactivation or over-expression of genes involved in glycogen synthesis or glycogen breakdown, respectively. This would liberate more carbon into biofuel production pathways. However, eliminating the cyanobacteria's ability to store glycogen was shown to adversely affect cell survival during the light to dark stage, as glycogen acts as a "stress buffer" during this energetically stressful transitions.[41] A genetically-engineered cyanobacterium that is incapable of accumulating glycogen would therefore be an unfit match for a biofuel platform that relies on the light-dark patterns of natural sunlight for an energy source. Unlocking these unused energy stores without causing detrimental effects to the organism is a key challenge that is still under investigation.

Increasing the rate of CO_2 fixed into reduced carbon is another approach in maximizing photosynthetic biofuel production. This can be accomplished by genetically targeting key areas in

carbon fixation. Some strategies include enhancing the efficiency of carbon fixation itself by over-expression of genes in Calvin-Benson cycle,[42] optimizing ribulose 1,5 bisphosphate carboxylase/oxygenase (RuBisCO) to its full catalytic potential through protein engineering,[43] or by designing new, more efficient carbon fixation pathways.[44] These approaches, though still in their infancy, hold great promise as future tools to increase biofuel production in photosynthetic organisms, while minimizing the energy input needed to maintain their overall metabolic state.

Conclusions

We have demonstrated the production of the cyclic hydrocarbon limonene using the photosynthetic cyanobacterium *Anabaena* sp. PCC 7120 by expressing a plant LimS individually and in combination with a synthetic *dxs-ipphp-gpps* operon. These cyanobacterial strains possess the ability to consecutively synthesize and release limonene into a culture headspace using atmospheric gases, light, and mineralized water, allowing for easy separation of the target compound from the culture biomass. Expressing the *dxs-ipphp-gpps* operon in conjunction with LimS resulted in an approximate 6.8-fold increase in limonene production under 150 $\mu E \cdot m^{-2} \cdot s^{-1}$ light, presumptively from an increased carbon flux into the MEP pathway. Under our experimental conditions, we achieved a maximum limonene productivity of 3.6±0.5 µg limonene$\cdot L^{-1} \cdot O.D.^{-1} \cdot hr^{-1}$ under 150 $\mu E \cdot m^{-2} \cdot s^{-1}$ light intensity. This production rate decreased dropped towards the end of the trial period, which we hypothesized is the result of poor light penetration in dense cultures ($O.D._{700\ nm}$>1.0). We observed that limonene production induces a positive effect on photosystem II activity. LimS-DXP *Anabaena* showed the highest PSII activity, that is about three times higher oxygen production than that in WT *Anabaena* (Fig. 5A). We hypothesize that because a new carbon sink in limonene synthesis has been added to the cyanobacterium, there is a greater pull of carbon from the Calvin cycle into the MEP pathway, creating a higher demand for ATP and NADPH to drive more CO_2-fixation. These energy equivalents are ultimately created from electrons harvested from water molecules, which results in the release of

oxygen gas from H_2O.

Limonene is an attractive choice for biofuel production, given its similar energy density, boiling point, and self-ignition temperature to petrodiesel.[10] The production of limonene from CO_2, mineralized water, and light using engineered cyanobacteria offers a promising way to produce biofuels while minimizing the human carbon footprint on the environment. To our knowledge, this is the first report of alkene-biofuel production from a filamentous, nitrogen-fixing cyanobacterium. Taken together, these results provide a first step in developing a large scale platform for limonene production using microbial photosynthesis.

Materials and Methods

Strains and growth conditions

Bacterial strains used in this study are listed in Table 1. All *E. coli* strains were grown in Luria-Bertani (LB) medium at 37°C, and 250 rpm. Kanamycin (Km; 50 $\mu g \cdot mL^{-1}$) and Ampicillin (Ap; 100 $\mu g \cdot mL^{-1}$) were used for antibiotic selection for *E. coli* during strain construction, and Neomycin (Nm; 100 $\mu g \cdot mL^{-1}$) was for transgenic *Anabaena* harboring cargo plasmids, respectively. Wild-type (WT) *Anabaena* cultures were grown in BG11 medium under constant white light (50 $\mu E \cdot m^{-2} \cdot s^{-1}$ at the culture surface using nine 15-inch, 15-watt fluorescent light bulbs) at 30°C and shaken at 120 rpm in a temperature controlled Innova 44R lighted incubator (New Brunswick Scientific). For increased light intensity experiments, the shaker was fitted with additional eight 24-inch, 17 watt fluorescent light bulbs to achieve an average light intensity of 150 $\mu E \cdot m^{-2} \cdot s^{-1}$. Light intensity was measured using a Li-Cor LI-190 Quantam sensor.

Plasmid Construction

All plasmids used in this study and details of their construction are listed in Table 1. Genes used in this study were PCR amplified with Phusion *Taq* polymerase (New England Biolabs), using forward and reverse primers (Table 2). The resultant PCR products were directly cloned into a pCR®2.1-TOPO® vector (TOPO TA Cloning® kit, Invitrogen). All cloned sequences were confirmed by sequencing, then excised and subcloned into pZR1188, a replicating shuttle vector for both *E. coli* and *Anabaena*, to produce cargo plasmids using standard molecular cloning protocols.[45]

Transfer of cargo plasmids into *Anabaena*

The transfer of pLimS and pLimS-DXP cargo plasmids into *Anabaena* was performed via bacterial conjugation using a bi-parental *E. coli* mating system[46] with the following modifications. *E. coli* HB101 bearing helper (pRL623) and conjugal (pRL443) plasmids were mated with *E. coli* NEB 10β harboring pLimS or pLimS-DXP, respectively, and selected on LB plates containing triple antibiotic selection for the three plasmids. Selected colonies were grown overnight in 2 mL of LB containing appropriate antibiotics, subcultured by adding 200 µL of overnight culture to 2 mL of fresh LB containing appropriate antibiotics, and grown for additional 3 hours. Cells were harvested by centrifugation at 3000×g, washed 3 times with 1 mL of LB to completely remove antibiotics, and resuspended with 200 µL LB and subjected for mating with *Anabaena*. A 10 mL culture of WT *Anabaena* was grown to early exponential stage ($O.D._{700\ nm}$ of 0.3) and then sonicated (Branson 1510 water bath sonicator) for 60-120 seconds to break filaments into 2-4 cell lengths, which were confirmed under light microscopy. Cells were harvested by centrifugation at 5,000×g for 10 minutes, resuspended in 200 µL of fresh BG11, and then mixed with above *E. coli* harboring triple plasmids for conjugal transfer. The above cell mixture was placed under lighted conditions at 25°C for 30 minutes, micro-pipetted on to an autoclaved Millipore Immobilon nitrocellulose filter (HATF08550) placed on a BG-11 plus 5% LB plate, and grown under white light for 3 days at 30°C. The filter was then

transferred to a BG11 plate containing Nm (100 μg·mL^{-1}) to select for positive exconjugants. Individual exconjugant colonies were further purified by restreaking onto fresh BG11 plates containing 100 μg·mL^{-1} Nm and routine colony PCR was used for verification of positive exconjugants.

Protein Extraction and Western Blot Analysis

Protein was extracted from both WT and LimS *Anabaena* cells to determine expression of LimS in the host strains. Ten-mL cultures were grown in BG11 with appropriate antibiotics until they reached mid exponential phase (O.D.$_{700\ nm}$ of 0.5), and the cells were pelleted and washed 3 times with sucrose buffer (50 mM Tris-HCl, 40 mM EDTA, 0.75 M sucrose) resuspended with 50 μL of lysis buffer (0.5 mg·mL^{-1} lysozyme, 10 μg·mL^{-1} DNAse I, and 10 μg·mL^{-1} RNase A.), and incubated at 37°C for 15 minutes. After incubation, 50 μL of 2×SDS loading buffer (50 mM Tris-HCl, pH 6.8, 4% SDS, 20% [vol/vol] glycerol, 200 mM dithiothreitol, 0.03% bromophenol blue) was added. The mixture was boiled for 5 minutes, and then centrifuged at 13,000 rpm for 10 minutes at 4°C. 5 μL protein extracts were loaded and separated by 12% SDS-PAGE at 200V for 30 minutes. The total proteins were transferred onto a PVDF membrane, and LimS-FLAG$_2$ was detected by Western blot using anti-FLAG (Sigma Aldrich) antibodies at a dilution of 1:5000. The membrane was then stained with Coomassie Blue R250 to visualize total proteins.

Limonene collection from culture headspace and GC-MS analysis

Starter cultures were set at O.D.$_{700\ nm}$ of 0.1 using a UV-Vis spectrophotometer (Genesys 10S, Thermo Scientific). LimS and LimS-DXP *Anabaena* strains were grown in 250 mL Erlenmeyer flasks containing 100 mL BG11 and 100 μg·mL^{-1} Nm, respectively, and bubbled with filtered air at a rate of 100 mL·min^{-1}. A small glass column filled with 100 mg of Supelpak 2SV resin (Sigma Aldrich) was attached to the exhaust port of each flask to capture limonene and other volatile metabolites from the

culture headspace. Resin samples from each flask were eluted twice with 2.5 mL of pentane containing 1 μg·mL^{-1} tetracosane as an internal standard (IS), pooled in 5 mL total volumes, evaporated to 1 mL using a gentle stream of N_2 gas (thus concentrating the IS to 5 μg·mL^{-1}), and subjected to gas chromatography-mass spectrometry (GC-MS) analysis (Agilent 7890A/5975C). One μL injected samples were separated using a HP-5MS column (35m×250μm×0.25μm), with H_2 as the carrier gas. The oven temperature was initially held at 40°C for 1 minute, increased 5°C·min^{-1} to 67°C and held for 3 min, increased 5°C·min^{-1} until 180°C was reached, and then further increased by 20°C·min^{-1} to 320°C. A set of limonene standards (Sigma Aldrich) at 0.1, 0.5, 1, 5, 10, 25, 50, and 100 μg·mL^{-1} in pentane were used to create a standard curve to quantify limonene captured by 2SV columns. To test absorption qualities of the 2SV resin, 10, 50 and 100 μg of limonene standard was spiked into 100 mL WT *Anabaena* cultures (O.D.$_{700\ nm}$ at 0.6) fitted with the 2SV column, and incubated in experimental growth conditions for three days, allowing limonene to volatilize and be collected by the 2SV columns. Limonene chromatograph peaks from the spiked cultures were then compared to the peaks generated from the standard curve to calculate the recovery rate of limonene. All measurements were performed in triplicate.

Chlorophyll extraction and analysis of photosynthetic activity

Chlorophyll was extracted using a 90% methanol extraction procedure described previously.[47] Oxygen evolution was quantified in 1 mL culture samples (adjusted to 10 μg·mL^{-1} chlorophyll) in BG11 with 1 mM $NaHCO_3$ using a Clark-type electrode and DW2 Oxygen Electrode Chamber with O_2 View Oxygen Monitoring software (Hansatech). Light was introduced to samples using an LS2/H Tungsten-halogen 100 W light source and adjusted with neutral density filters. Light intensity and sample temperature was monitored using a Quantitherm light-temperature meter during experimentation. All measurements were performed in triplicate.

Large-Scale Limonene Productivity and Cost Calculations

Theoretical limonene yield was calculated by balancing the stoichiometry of 10 CO_2 and 8 H_2O to one limonene molecule ($C_{10}H_{16}$) and 14 O_2, creating 136.23 g limonene for every 440.1 g of CO_2. Thus, 2.75 million kg of CO_2 (1% of annual emissions from one ethanol plant) could generate 852500 $kg \cdot yr^{-1}$ (1013674 L based on limonene density of 0.841 kg/L), and would require a productivity of 55.5 $mg \cdot L^{-1} \cdot hr^{-1}$ from a 10-hectare greenhouse producing 8 $hr \cdot d^{-1}$, 300 $d \cdot yr^{-1}$, with 6.4 million L of photobioreactor fluid. Total limonene production costs were calculated by assuming similar production costs to a corn ethanol plant. Capital costs: $\$0.50 \cdot L^{-1}$; Labor: \$50000 × 6 people = $\$300000 \cdot yr^{-1} / 1013674\ L \cdot yr^{-1} = \$0.30 \cdot L^{-1}$; Operation costs: $\$0.50 \cdot L^{-1}$.

Acknowledgments

The authors would like to thank Dr. William Gibbons for making a valuable contribution to the interactive discussion and for many helpful suggestions. This work was partially supported by the National Science Foundation, Energy for Sustainability Grant No. 1133951 (to R.Z.), North Central Sun Grant/DOT award No. 3FB249 (to R.Z.) and by South Dakota Agricultural Experiment Station. The authors would like to thank Joerg Bohlmann for gift of pET101-LimS, Jay Keasling for pSOE4, and Reuben Peters for pDEST17-Rv0989c. We thank David Sturdevant and Thor Lammers for their assistance in the construction of pZR1460 and pZR1241. We would also like to acknowledge use of the South Dakota State University Functional Genomics Core Facility supported in part by NSF/EPSCoR Grant No. 0091948 and by the State of South Dakota.

Notes and references

[a] *Department of Biology & Microbiology, South Dakota State University, Brookings, SD, 57007 USA.*

* Corresponding author; *E-mail: ruanbao.zhou@sdstate.edu; Fax: +1 605 688 5624; Tel: +1 605 688 5259*

1. T. Grawert, M. Groll, F. Rohdich, A. Bacher and W. Eisenreich, *Cell Mol Life Sci*, 2011, **68**, 3797-3814.
2. L. S. Zhao, W. C. Chang, Y. L. Xiao, H. W. Liu and P. H. Liu, *Annu Rev Biochem*, 2013, **82**, 497-+.
3. F. Chen, D. Tholl, J. Bohlmann and E. Pichersky, *Plant Journal*, 2011, **66**, 212-229.
4. J. Degenhardt, T. G. Kollner and J. Gershenzon, *Phytochemistry*, 2009, **70**, 1621-1637.
5. M. Fellermeier, M. Raschke, S. Sagner, J. Wungsintaweekul, C. A. Schuhr, S. Hecht, K. Kis, T. Radykewicz, P. Adam, F. Rohdich, W. Eisenreich, A. Bacher, D. Arigoni and M. H. Zenk, *Eur J Biochem*, 2001, **268**, 6302-6310.
6. E. Vranova, D. Coman and W. Gruissem, *Mol Plant*, 2012, **5**, 318-333.
7. T. C. R. Brennan, C. D. Turner, J. O. Kromer and L. K. Nielsen, *Biotechnol Bioeng*, 2012, **109**, 2513-2522.
8. W. A. Duetz, H. Bouwmeester, J. B. van Beilen and B. Witholt, *Applied microbiology and biotechnology*, 2003, **61**, 269-277.
9. P. Hellier, L. Al-Haj, M. Talibi, S. Purton and N. Ladommatos, *Fuel*, 2013, **111**, 670-688.
10. A. Langlois and O. Lebel, *Energ Fuel*, 2010, **24**, 5257-5263.
11. R. Kummer, F. C. Fachini-Queiroz, C. F. Estevao-Silva, R. Grespan, E. L. Silva, C. A. Bersani-Amado and R. K. Cuman, *Evidence-based complementary and alternative medicine : eCAM*, 2013, **2013**, 859083.
12. S. S. Jia, G. P. Xi, M. Zhang, Y. B. Chen, B. Lei, X. S. Dong and Y. M. Yang, *Oncol Rep*, 2013, **29**, 349-354.
13. J. A. Miller, J. E. Lang, M. Ley, R. Nagle, C. H. Hsu, P. A. Thompson, C. Cordova, A. Waer and H. H. S. Chow, *Cancer Prev Res*, 2013, **6**, 577-584.
14. A. M. Ruffing, *Bioengineered Bugs*, 2011, **2**, 136-149.
15. D. C. Ducat, J. C. Way and P. A. Silver, *Trends Biotechnol*, 2011, **29**, 95-103.
16. J. Yang, Q. Nie, M. Ren, H. Feng, X. Jiang, Y. Zheng, M. Liu, H. Zhang and M. Xian, *Biotechnology for biofuels*, 2013, **6**, 60.
17. K. K. Reiling, Y. Yoshikuni, V. J. Martin, J. Newman, J. Bohlmann and J. D. Keasling, *Biotechnol Bioeng*, 2004, **87**, 200-212.
18. G. P. Ghimire, H. C. Lee and J. K. Sohng, *Appl Environ Microbiol*, 2009, **75**, 7291-7293.
19. C. Wang, S. H. Yoon, H. J. Jang, Y. R. Chung, J. Y. Kim, E. S. Choi and S. W. Kim, *Metab Eng*, 2011, **13**, 648-655.
20. J. Alonso-Gutierrez, R. Chan, T. S. Batth, P. D. Adams, J. D. Keasling, C. J. Petzold and T. S. Lee, *Metab Eng*, 2013, **19C**, 33-41.
21. P. Lindberg, S. Park and A. Melis, *Metab Eng*, 2010, **12**, 70-79.
22. K. Takahama, M. Matsuoka, K. Nagahama and T. Ogawa, *Journal of Bioscience and Bioengineering*, 2003, **95**, 302-305.
23. J. Ungerer, L. Tao, M. Davis, M. Ghirardi, P. C. Maness and J. P. Yu, *Energ Environ Sci*, 2012, **5**, 8998-9006.
24. J. W. K. Oliver, I. M. P. Machado, H. Yoneda and S. Atsumi, *Proceedings of the National Academy of Sciences of the United States of America*, 2013, **110**, 1249-1254.
25. S. Atsumi, W. Higashide and J. C. Liao, *Nat Biotechnol*, 2009, **27**, 1177-U1142.
26. D. C. Ducat, J. A. Avelar-Rivas, J. C. Way and P. A. Silver, *Appl Environ Microb*, 2012, **78**, 2660-2668.
27. H. Masukawa, K. Inoue, H. Sakurai, C. P. Wolk and R. P. Hausinger, *Appl Environ Microb*, 2010, **76**, 6741-6750.
28. J. Peccia, B. Haznedaroglu, J. Gutierrez and J. B. Zimmerman, *Trends Biotechnol*, 2013, **31**, 134-138.
29. J. C. F. Ortiz-Marquez, M. Do Nascimento, M. D. Dublan and L. Curatti, *Appl Environ Microb*, 2012, **78**, 2345-2352.
30. K. Okada and T. Hase, *J Biol Chem*, 2005, **280**, 20672-20679.
31. A. Byun-McKay, K. A. Godard, M. Toudefallah, D. M. Martin, R. Alfaro, J. King, J. Bohlmann and A. L. Plant, *Plant Physiol*, 2006, **140**, 1009-1021.
32. F. K. Bentley, J. G. Garcia-Cerdan, H. C. Chen and A. Melis, *Bioenerg Res*, 2013, **6**, 917-929.
33. F. K. Bentley and A. Melis, *Biotechnol Bioeng*, 2012, **109**, 100-109.
34. V. J. J. Martin, D. J. Pitera, S. T. Withers, J. D. Newman and J. D. Keasling, *Nat Biotechnol*, 2003, **21**, 796-802.

35. Y. Chisti, *Trends Biotechnol*, 2008, **26**, 126-131.

36. J.W. Richardson, J.L. Outlaw and M. Allison, *AgBioForum*, 2010, **3**, 119-130.

37. B. Green, N. Reppas and D. Robertson, Joule Biotechnologies, Ethanol production by microorganisms, U.S. patent 7,968,321.

38. C. V. G. Lopez, F. G. A. Fernandez, J. M. F. Sevilla, J. F. S. Fernandez, M. C. C. Garcia and E. M. Grima, *Bioresource technology*, 2009, **100**, 5904-5910.

39. H. Qiang, Y. Zarmi and A. Richmond, *Eur J Phycol*, 1998, **33**, 165-171.

40. J.C. Yang and J.H. Zhang, *J Exp Bot*, 2010, **61**, 3177-3189.

41. M. Grundel, R. Scheunemann, W. Lockau and Y. Zilliges, *Microbiol-Sgm*, 2012, **158**, 3032-3043.

42. Y. Miyagawa, M. Tamoi and S. Shigeoka, *Nat Biotechnol*, 2001, **19**, 965-969.

43. M. A. J. Parry, P. J. Andralojc, J. C. Scales, M. E. Salvucci, A. E. Carmo-Silva, H. Alonso and S. M. Whitney, *J Exp Bot*, 2013, **64**, 717-730.

44. A. Bar-Even, E. Noor, N. E. Lewis and R. Milo, *Proceedings of the National Academy of Sciences of the United States of America*, 2010, **107**, 8889-8894.

45. M. R. Green and J. Sambrook, *Molecular cloning : a laboratory manual*, Cold Spring Harbor Laboratory Press, Cold Spring Harbor, N.Y., 2012.

46. J. ElhaI, A. Vepritskiy, A. M. MuroPastor, E. Flores and C. P. Wolk, *J Bacteriol*, 1997, **179**, 1998-2005.

47. J. C. Meeks and R. W. Castenholz, *Archiv fur Mikrobiologie*, 1971, **78**, 25-41.

48. K. Chen, L. Gu, X. Xiang, M. Lynch and R. Zhou, *J Bacteriol*, 2012, **194**, 6105-6115.

49. X. Xiang, L. Gu, D. Raynie, W. Gibbons and R. Zhou, Proceedings from Sun Grant National Conference: Science for Biomass Feedstock Production and Utilization, 2012, 2, 3.17.

50. F. M. Mann, J. A. Thomas and R. J. Peters, *Febs Lett*, 2011, **585**, 549-554.

Table 1 Plasmids and Strains used in this study

Plasmids	Relevant Characteristics	Construction	Source
pRL443	Amp^r, Tc^r; Conjugal plasmid		Elhai et al.[46]
pRL623	Cm^r; Helper plasmid		Elhai et al.[46]
pZR618	Amp^r; T_7; MCS; His_6; F_2		Chen et al.[48]
pZR807	Km^r, Nm^r; P_{nir}/P_{psbA1}; MCS		Gu et al.[48]
pZR1188	Km^r, Nm^r; P_{nir}/P_{psbA1}; MCS; F_2	BglII-T_7-MCS-F_2-XhoI fragment excised from pZR618, subcloned into BamHI-SalI digested pZR807	This study
pET101-LimS	Amp^r; T_7; *lims* from *Picea sitchensis*		Byun-McKay et al.[31]
pZR1240	Km^r, Amp^r; P_{lac}/T_7; *lims*	*lims* PCR amplified from pET101-LimS using primers ZR490 and 491 and cloned into pCR®2.1-TOPO®	This study
pLimS	Km^r, Nm^r; P_{nir}/P_{psbA1}; *lims*-F_2	BglII-*lims*-SalI fragment excised from pZR1240, subcloned into BglII-SalI-digested pZR1188	This study
pDEST17-*Rv0989c*	Amp^r; T_7; *gpps*		Mann et al.[50]
pZR1541	Km^r, Amp^r; P_{lac}/T_7; *gpps*	*gpps* PCR amplified from pDEST17-*Rv0989c* using primers ZR762 and 763 and cloned into pCR®2.1-TOPO®	This study
pZR1546	Km^r, Nm^r; P_{nir}/P_{psbA1}; *gpps*	BamHI-*gpps*-XhoI fragment excised from pZR1541 and subcloned into BamHI-SalI digested pZR1188	This study
pSOE4	Cm^r; P_{lac}; *dxs-ipphp-ispA*		Martin et al.[34]
pZR1460	Km^r, Amp^r; P_{lac}/T_7; *dxs-ipphp*	*dxs-ipphp* PCR amplified from pSOE4 using primers ZR864 and 865 and cloned into pCR®2.1-TOPO®	This study
pZR1461	Km^r, Nm^r; P_{nir}/P_{psbA1}; *dxs-ipphp*	XhoI-*dxs-ipphp*-BamHI fragment excised from pZR1460 and subcloned into XhoI-BamHI digested pZR1188	This study
pZR1462	Km^r, Nm^r; P_{nir}/P_{psbA1}; *dxs-ipphp-gpps*	BamHI-*gpps*-NotI fragment excised from pZR1546, subcloned into BamHI-NotI digested pZR1461	This study
pLimS-DXP	Km^r, Nm^r; P_{nir}/P_{psbA1}; *lims-dxs-ipphp-gpps*	XhoI-*dxs-ipphp-gpps*-NotI fragment excised from pZR1462and subcloned into SalI-NotI-digested pLimS	This study

Strains	Relevant Characteristics	Source
One Shot® Top10 *E. coli*	Cloning host	Invitrogen
NEB 10-beta *E. coli*	Cloning host	New England Biolabs
HB101 *E. coli*	For conjugal transfer of cargo plasmids into *Anabaena* sp. PCC 7120	This study
Anabaena sp. PCC 7120	Wild-type *Anabaena* sp. PCC 7120	This study
LimS *Anabaena*	*Anabaena* sp. PCC 7120 carrying pLimS plasmid	This study
LimS-DXP *Anabaena*	*Anabaena* sp. PCC 7120 carrying pLimS-DXP plasmid	This study

Acronyms: Amp^r, ampicillin resistance; Tc^r, tetracycline resistance; Cm^r, chloramphenicol resistance; Km^r, kanamycin resistance; Nm^r, neomycin resistance; His_6, Histidine×6 tag; F_2, FLAG×2 tag; P_{nir}, nitrate promoter; P_{psbA1}, psbA1 promoter; T_7, T_7 promoter; P_{lac}, lac promoter.

Table 2 Primers used in this study

Name	Sequence (5' to 3")	Source
ZR490	AGATCTcaaagacgcagaggcaattat	This study
ZR491	AGTCGACcaaagtcacaggttcaaggacc	This study
ZR762	T**GGATCC**Tatgatcccggcagtcagcctgg	This study
ZR763	T**CTCGAG**gtcgcacgcagatatcgcgtggtc	This study
ZR864	T**CTCGAG**TA*A*GGAGGAATTCACCatgagtt	This study
ZR865	T**GGATCC**TCA*TCCTCC*gttgatgtgatgc	This study

Bolded letters refer to engineered restriction sites; italicized letters refer to engineered ribosomal binding sites (RBS); underlined letters refer to engineered stop codons; lowercase letters refer to gene sequence found in nature.

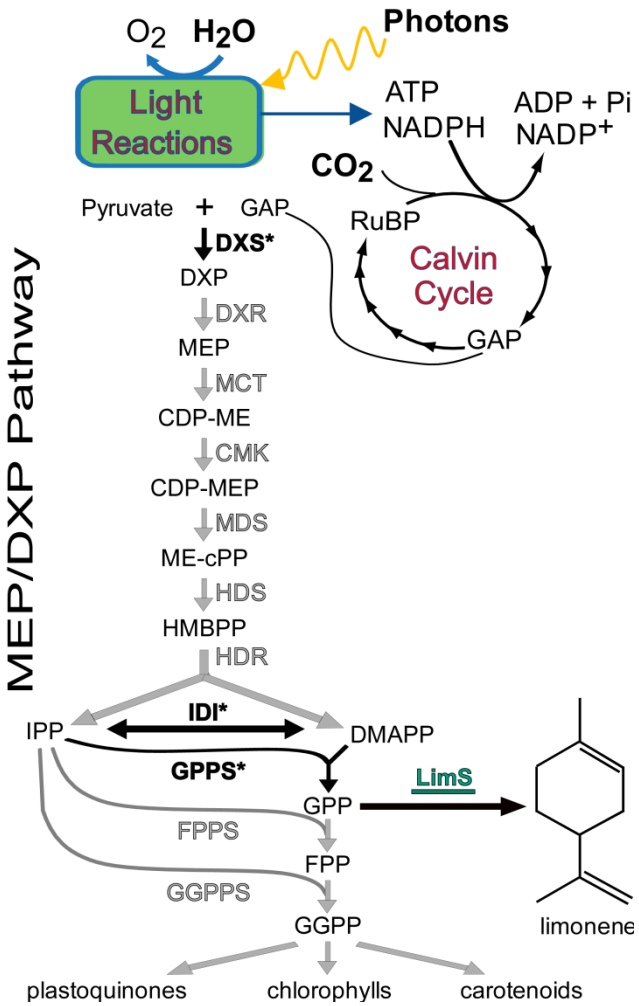

Fig. 1 The limonene production pathway in engineered cyanobacteria. MEP pathway enzymes over-expressed in *Anabaena* are marked with asterisks. The heterogously expressed LimS is underlined. Abbreviations used: GAP, glyceraldhyde 3-phosphate; RuBP, ribulose-1,5-bisphosphate; DXP, 1-deoxy-D-xylulose 5-phosphate; MEP, methylerythritol-4-phosphate; CDP-ME diphosphocytidylyl methylerythritol; CDP-MEP, methylerythritol-2-phosphate; ME-cPP, methylerythritol-2,4-cyclopyrophosphate; HMBPP, hydroxymethylbutenyl pyrophosphate; IPP, isopentlyl pyrophosphate; DMAPP, dimethylallyl pyrophosphate; GPP, geranyl pyrophosphate; FPP, farnesyl pyrophosphate; GGPP geranylgeranyl pyrophosphate; DXS, DXP synthase; DXR, DXP reductoisomerase; MCT, CDP-ME synthase; CMK, CDP-ME kinase; MDS, ME-cPP synthase; HDS, HMBPP synthase; HDR, HMBPP reductase; IDI, IPP:DMAPP isomerase; GPPS, GPP synthase; LimS, limonene synthase; FPPS, FPP synthase; GGPPS, GGPP synthase.

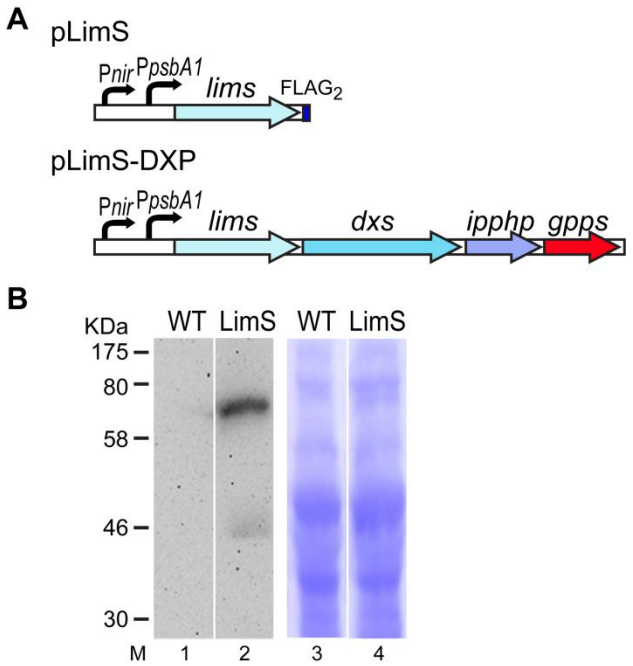

Fig. 2 Expression of limonene synthase in *Anabaena*. (A) Schematic of pLimS and pLimS-DXP constructs with promoters (P_{nir}/P_{psbA1}), genes (*lims* or *lims-dxs-ipphp-gpps* operon, respectively), and $FLAG_2$ epitope tag labeled. (B) Western blot analysis revealed a 69 kDa LimS-$FLAG_2$ protein in LimS *Anabaena* bearing pLimS plasmid (lane 2), but absent in the WT sample (lane 1). The same PVDF membrane was stained with Coomassie blue R250 (lanes 3 and 4) to show equal protein loading.

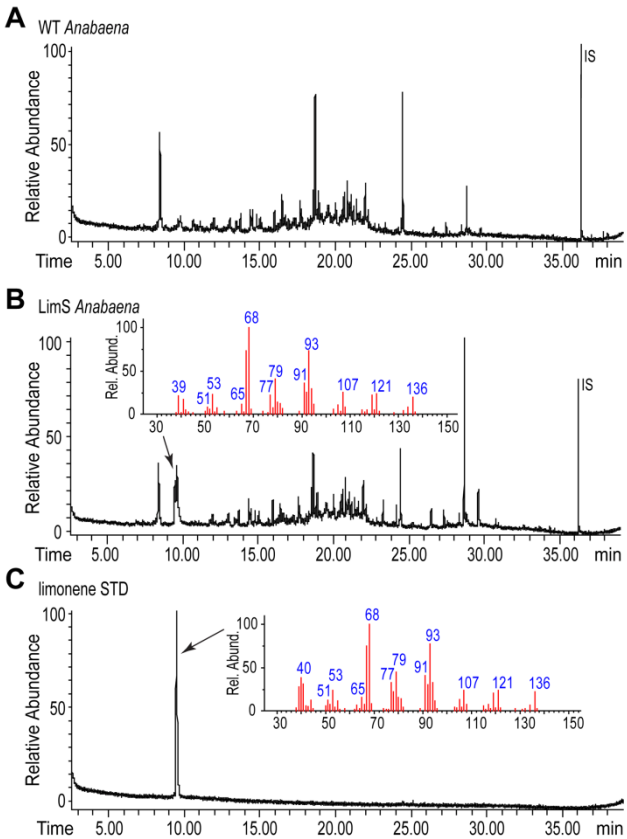

Fig. 3 GC-MS chromatographs of flask headspace samples from WT (A) and LimS (B) *Anabaena* cultures. A peak at the retention time 9.47 minutes (arrowed) found in LimS *Anabaena* matches the limonene standard (C), but is absent in the WT (A). Mass spectra (insert figures) of these peaks also display the expected pattern for limonene. Five $\mu g \cdot mL^{-1}$ tetracosane serves as an internal standard (IS).

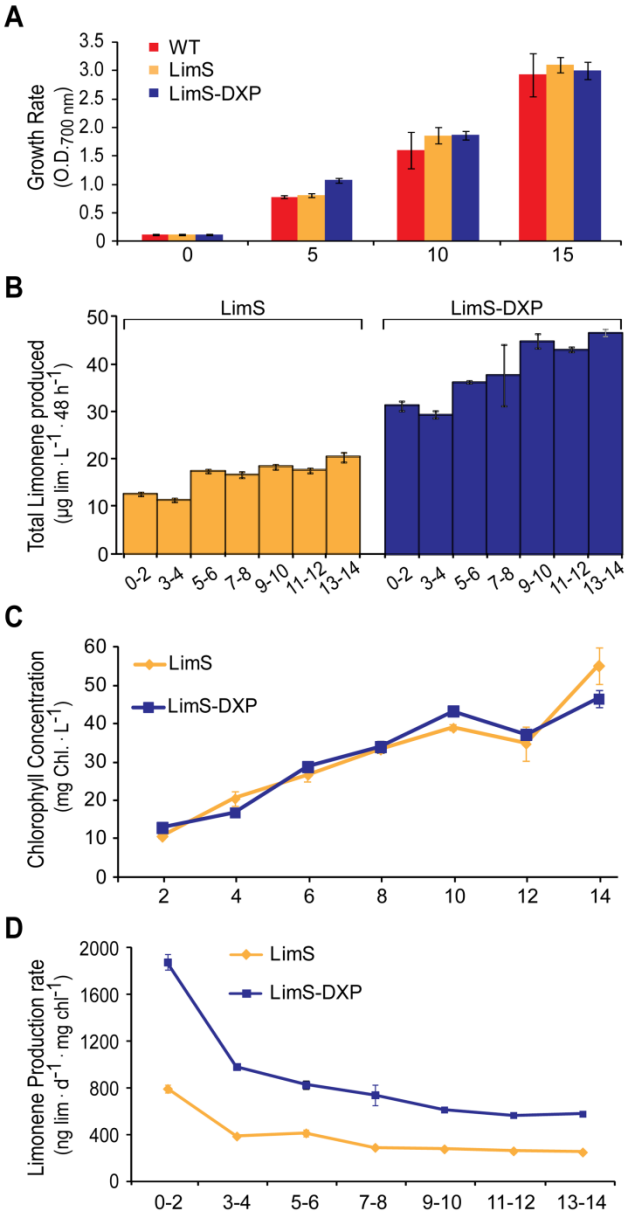

Fig. 4 Growth and limonene production characteristics of genetically engineered *Anabaena* strains. (A) Similar growth rates revealed for WT, LimS, and LimS-DXP *Anabaena* as indicated by optical density readings at 700 nm ($O.D._{700\ nm}$). (B) Total limonene captured in 2SV column for 48 hours from LimS and LimS-DXP *Anabaena* culture flasks, respectively. (C) Chlorophyll concentration of LimS and LimS-DXP *Anabaena* during 14 day growth experiment. (D) Rate of limonene produced from LimS and LimS-DXP *Anabaena* per mg of chlorophyll. The horizontal axis represents time (day). All experiments performed under 50 $\mu E \cdot m^{-2} \cdot s^{-1}$ light conditions. Results are the average of three biological replicates, with error bars representing the standard deviation of the mean.

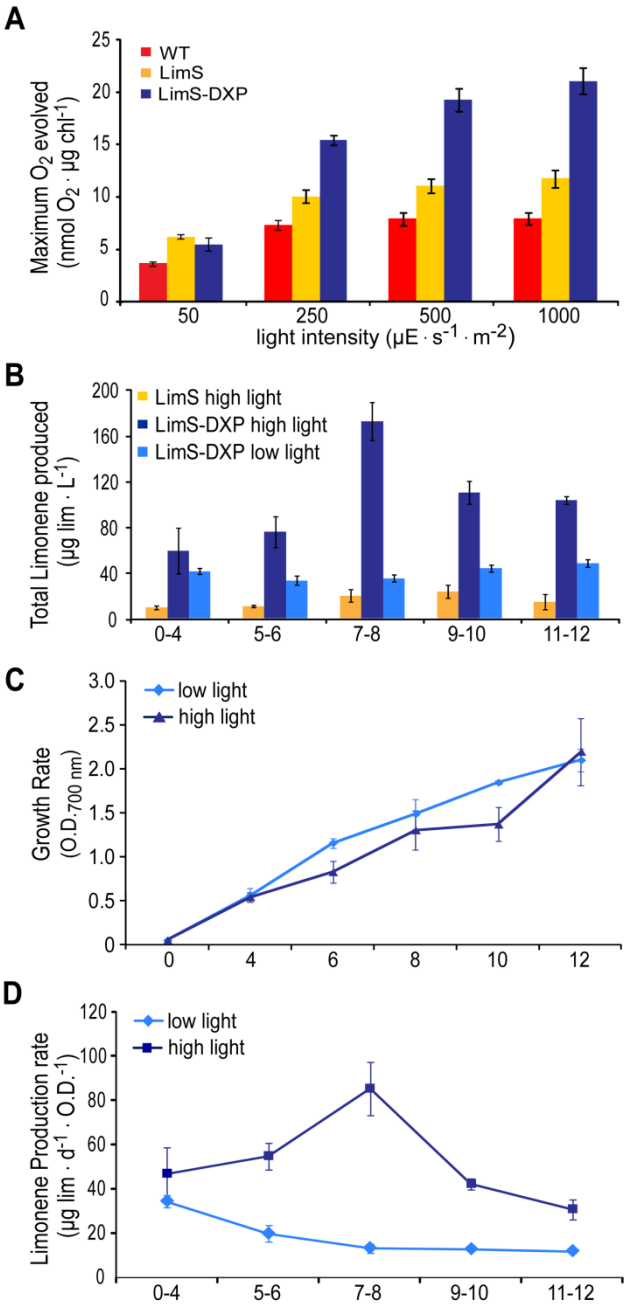

Fig. 5 Increasing light intensity improves limonene production in *Anabaena*. (A) Maximum oxygen evolution under indicated light conditions for 10-15 min was determined using 10 µg chlorophyll in 1 mL BG11 containing 1 mM $NaHCO_3$. (B) Limonene yield from LimS and LimS-DXP *Anabaena* under low (50 $\mu E \cdot m^{-2} \cdot s^{-1}$) and high (150 $\mu E \cdot m^{-2} \cdot s^{-1}$) light conditions during the period of time indicated in X-axis. (C) Cell densities ($O.D._{700nm}$) of LimS-DXP *Anabaena* during 12 day growth trial under low (50 $\mu E \cdot m^{-2} \cdot s^{-1}$) and high (150 $\mu E \cdot m^{-2} \cdot s^{-1}$) light conditions. (D) Limonene production rate of

LimS-DXP under low (50 $\mu E \cdot m^{-2} \cdot s^{-1}$) and high (150 $\mu E \cdot m^{-2} \cdot s^{-1}$) light conditions. The horizontal axis of (B), (C), and (D) represents time (day). Results are the average of three biological replicates, with error bars representing the standard deviation of the mean.